RESEARCH ARTICLE

Syndecan-1-Induced ECM Fiber Alignment Requires Integrin αvβ3 and Syndecan-1 Ectodomain and Heparan Sulfate Chains

Ning Yang[1], Andreas Friedl[1,2,3]*

1 Department of Pathology and Laboratory Medicine, University of Wisconsin-Madison, Madison, Wisconsin, United States of America, 2 Pathology and Laboratory Medicine Service, William S. Middleton Memorial Veterans Hospital, Department of Veterans Affairs Medical Center, Madison, Wisconsin, United States of America, 3 UW Carbone Cancer Center, Madison, Wisconsin, United States of America

* afriedl@wisc.edu

Abstract

Expression of the cell surface proteoglycan syndecan-1 (Sdc1) is frequently induced in stromal fibroblasts of invasive breast carcinomas. We have recently identified a correlation between stromal Sdc1 expression and extracellular matrix (ECM) fiber alignment, both *in vitro* and *in vivo*. ECMs derived from Sdc1-positive human mammary fibroblasts (HMF) showed an aligned fiber architecture, which contrasted markedly with the more random fiber arrangement in the ECM produced by Sdc1-negative HMFs. We further demonstrated that aligned fiber architecture promotes the directional migration and invasion of breast carcinoma cells. To decipher the molecular mechanisms governing the formation of an aligned, invasion-permissive ECM, a series of Sdc1 mutants was introduced into HMF. We found that both the ectodomain and heparan sulfate chains of Sdc1 were required for full activity of Sdc1 in regulating ECM alignment, while transmembrane and cytoplasmic domains were dispensable. Sdc1 regulates the activities of several integrins via its ectodomain. Integrins are key players in the assembly of fibronectin-rich ECM. In addition, integrins are capable of regulating cell morphology and cell shape and orientation may affect ECM architecture. Therefore, we investigated the role of integrins in Sdc1-mediated ECM fiber alignment. Sdc1-overexpressing HMF gained an enhanced spindle-shaped morphology when cultured in an overconfluent state under conditions permissive for ECM production, which was partially reversed by siRNA-mediated silencing of β3 integrin expression. Moreover, suppression of αvβ3 integrin activity by a function-blocking antibody or β3 knockdown largely abolished the aligned ECM fiber architecture and consequently the invasion-permissive properties of the ECM induced by Sdc1. The results suggest that Sdc1 may modulate fibronectin fibrillogenesis and/or alter cell morphology during ECM production through αvβ3 integrin, thereby mediating ECM fiber alignment. Understanding the mechanisms governing ECM organization may lead to the development of novel stroma-targeted therapy for breast cancer, aiming at converting an invasion-permissive to an invasion-restrictive microenvironment.

Introduction

During carcinogenesis, the malignant epithelium and the stroma co-evolve and alterations in cancer stroma contribute to the malignant phenotype. A major acellular component of the tumor stroma is the extracellular matrix (ECM), a three-dimensional (3D) network of proteins, glycoproteins, proteoglycans and polysaccharides. In addition to serving as a structural scaffold, the ECM regulates a wide variety of key cellular events including adhesion, migration, proliferation, differentiation and survival (for reviews see [1,2]). Under normal physiological conditions, the ECM dynamics (production, remodeling and degradation) are precisely regulated to ensure normal organ development and tissue homeostasis. In many cancer types, abnormal deposition of ECM components, resulting in alterations in the biochemical properties of the ECM that promote cancer progression, has been observed [3,4]. Recent evidence indicates that the physical properties of the ECM such as rigidity, topography and architecture are also altered in cancers and that these changes may play key roles in facilitating cancer invasion and progression [5–13]. The fibroblast is the major contributor to the synthesis and remodeling of the ECM and is a prevalent cell type within the tumor stroma. To date, the molecular mechanisms by which the stromal fibroblasts modulate the topography and fine structure of the ECM remain largely unknown.

Sdc1 belongs to a four-member family of cell surface heparan sulfate proteoglycans (HSPGs) [14]. Sdc1 is composed of a transmembrane core protein and covalently coupled heparan sulfate (HS) and chondroitin sulfate (CS) glycosaminoglycan (GAG) chains. Via its HS chains, Sdc1 interacts with a wide range of molecules, functions as a co-receptor to a variety of growth factors and interacts with a number of ECM components. Via its core protein, Sdc1 regulates the activities of integrins and associates with the actin cytoskeleton (for reviews see [15,16]). Consequently, Sdc1 regulates cell proliferation, adhesion, migration, cytoskeletal organization and mediates cell-cell and cell-ECM interactions. In adult organisms, Sdc1 is expressed predominantly by epithelial cells and mature plasma cells, although it is also found in mesenchymal cells and lymphoid cells during development [17–19]. Dysregulated expression of Sdc1 has been reported in many types of cancers and been linked to cancer cell proliferation, invasion, metastasis, angiogenesis, and predicts poor prognosis [20–24].

Our previous work indicated that stromal Sdc1 functions as a critical regulator of ECM architecture [25]. Sdc1 is frequently aberrantly expressed by stromal fibroblasts in invasive breast carcinomas [26,27]. *In vivo* and *in vitro*, stromal syndecan-1 expression correlates with a dramatically altered ECM fiber architecture. ECMs produced by Sdc1-expressing human mammary fibroblasts show an organized, aligned fiber architecture, which contrasts markedly with the haphazard fiber arrangement observed in the ECM produced by Sdc1-negative fibroblasts. Moreover, the structurally abnormal ECM derived from Sdc1-positive fibroblasts promotes the directional migration and invasion of the breast carcinoma cells [25].

In the present study, we identify the molecular regions within Sdc1 that are essential for its activity as an ECM organizer. We find that both the ectodomain and HS chains of Sdc1 are required for the production of aligned ECM fiber architecture. In addition, we show that activity of the integrin αvβ3 is not only involved in Sdc1-induced spindle-shaped morphology of fibroblasts but also required for Sdc1-dependent ECM fiber alignment. We propose that Sdc1 may modulate fibronectin fibrillogenesis through both direct and indirect mechanisms and/or regulate cell morphology, thereby mediating ECM fiber alignment.

Results

The Sdc1 ectodomain and HS chains are required for ECM alignment

We have shown previously that Sdc1 functions as a critical regulator during ECM production and that Sdc1-expressing human mammary fibroblasts which are frequently found in the

stroma of human breast carcinomas give rise to an aligned, invasion-permissive ECM [25]. To decipher the molecular mechanisms by which Sdc1 modulates the ECM architecture, we first set out to identify the functional domains of Sdc1 that are required for its activity as an ECM organizer. The Sdc1 molecule consists of a core protein and covalently attached GAG chains, three of which are HS chains near the N-terminus. The core protein of Sdc1 can be divided into 3 functional domains: the extracellular domain (ectodomain), the transmembrane domain and the cytoplasmic domain. HMF were stably transfected with a series of Sdc1 mutants and the ECMs produced by these cells were compared to ECMs produced by mock-transfected (negative control) or wild-type Sdc1-transfected HMF. These Sdc1 mutants (schematically shown in Fig 1A) include Sdc1-ΔHS (a HS-deficient mutant in which the three serine residues S37, S45, and S47 required for HS chain attachment are mutated to alanines) [28], Sdc1-TMM (a transmembrane domain substitution mutant in which all the amino acid residues of the transmembrane domain are replaced with leucine residues) [29], Sdc1-ΔCyto (a cytoplasmic domain deletion mutant in which all but the first amino acid residue of the cytoplasmic domain are deleted) [30], and Sdc1-ΔEcto (an ectodomain truncation mutant in which all but the 87 N-terminal amino acids of the extracellular domain are deleted while the three HS chain attachment sites remain unaffected) [31,32]. Populations of HMF expressing these Sdc1 mutant proteins at levels similar to wild-type Sdc1 were enriched by fluorescence-activated cell sorting (FACS) and the expression levels were confirmed by flow cytometry (Fig 1B).

The architecture of the 3D ECMs produced by these fibroblasts was examined by confocal microscopy of fibronectin (FN)-immunolabeled ECM preparations (Fig 2A). The expression of Sdc1 greatly affected the topography of the fibroblast-derived ECMs. Consistent with our previous findings, HMF expressing wild-type Sdc1 generated an ECM (ECM-Sdc1) with an organized, parallel FN fiber orientation, which contrasted dramatically with the haphazard fiber arrangement in the ECM produced by the Sdc1-negative HMF (ECM-mock). The transmembrane and cytoplasmic domains of Sdc1 were dispensable for Sdc1-mediated ECM alignment, since fibers in the ECMs derived from HMF that expressed Sdc1-ΔCyto and Sdc1-TMM (ECM-Sdc1-ΔCyto and ECM-Sdc1-TMM) were organized in parallel patterns closely resembling those in ECM-Sdc1. In contrast, HMF that express Sdc1-ΔEcto or Sdc1-ΔHS generated ECMs (ECM-Sdc1-ΔEcto and ECM-Sdc1-ΔHS) with random fiber arrangement, indicating that the Sdc1 HS chain and the part of the ectodomain located between the HS attachment sites and transmembrane domain are required for its full activity as an ECM organizer. Quantitative analysis confirmed that the mean fiber-to-fiber angles in ECM-Sdc1-ΔEcto and ECM-Sdc1-ΔHS are significantly larger than those in ECM-Sdc1 (p<0.001 for both ECM-Sdc1-ΔEcto and ECM-Sdc1-ΔHS) and statistically indistinguishable from ECM-mock. The mean fiber-to-fiber angles in ECM-Sdc1-ΔCyto and ECM-Sdc1-TMM are not significantly different from those in ECM-Sdc1 (Fig 2B).

We and others had previously determined that mammary fibroblast-derived ECMs with an aligned fiber architecture promote the directionally persistent migration of breast carcinoma cells [11,25]. Therefore, we analyzed the migration of 2 breast carcinoma cell lines, MDA-MB-231, highly invasive, triple-negative cells and MCF10DCIS.com, a model of ductal carcinoma in situ, within the different ECMs using a time-lapse motility assay (Fig 3A). Indeed, in cell-free ECM-Sdc1-ΔHS and ECM-Sdc1-ΔEcto, the majority of carcinoma cells migrated in apparently random and changing directions, similar to the movement observed in ECM-mock. The directionality of migration (which was calculated as the ratio of net distance between starting point and end point to the total distance traveled) of MDA-MB-231 and MCF10DCIS.com cells in these three ECMs had values of less than 0.5. In contrast, both breast carcinoma cell lines migrated with significantly more persistent directionality in ECM-Sdc1. We also examined the invasion of the 2 breast carcinoma cell lines through the different cell-derived ECMs
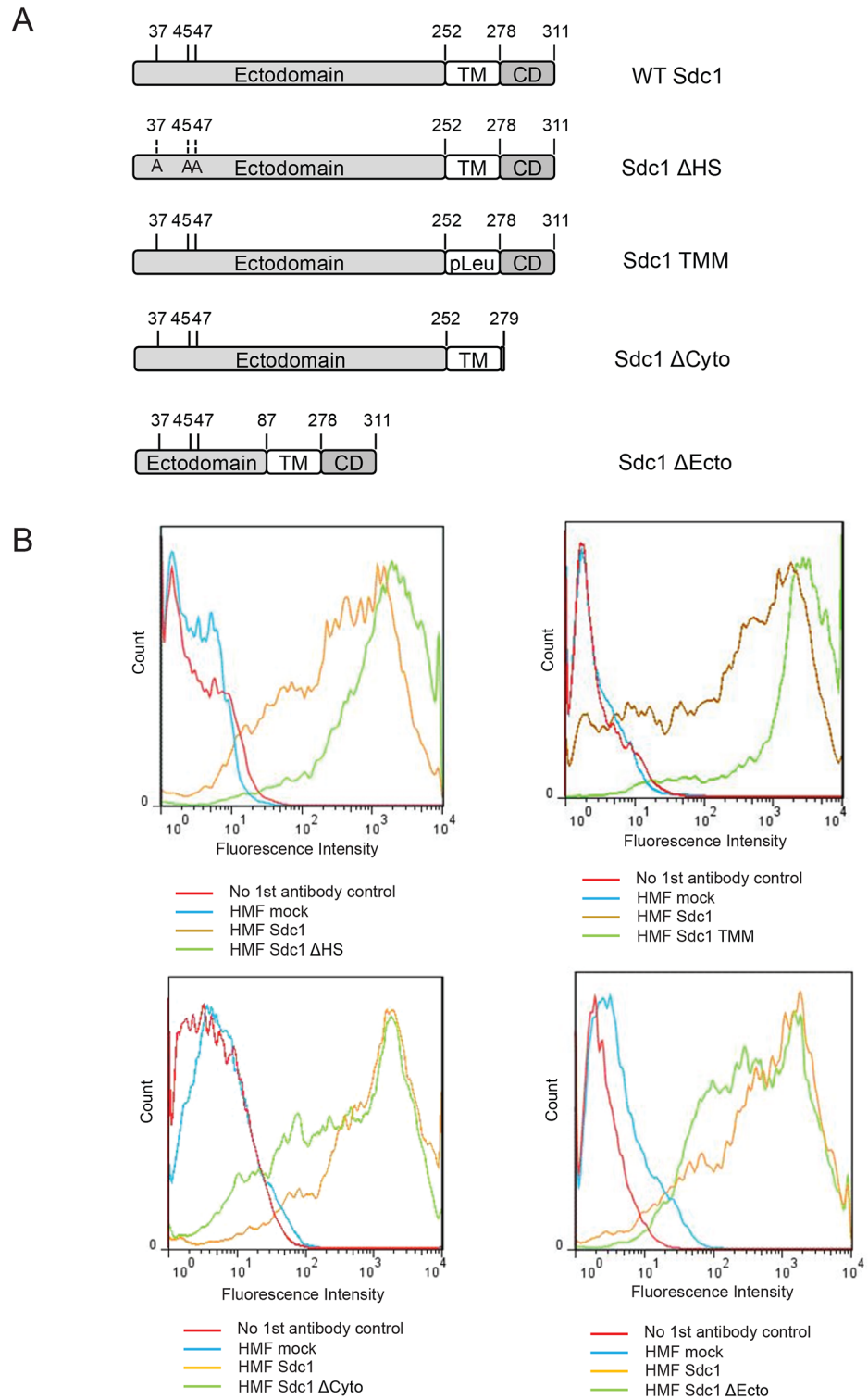
Fig 1. Generation of stable HMF cell lines expressing mutant forms of Sdc1. A) Schematic representation of Sdc1 mutant constructs introduced into HMF cells. B) Flow cytometry analysis of exogenous Sdc1 in stably transfected HMF reveals that wildtype Sdc1 and Sdc1 mutants are expressed at comparable levels.
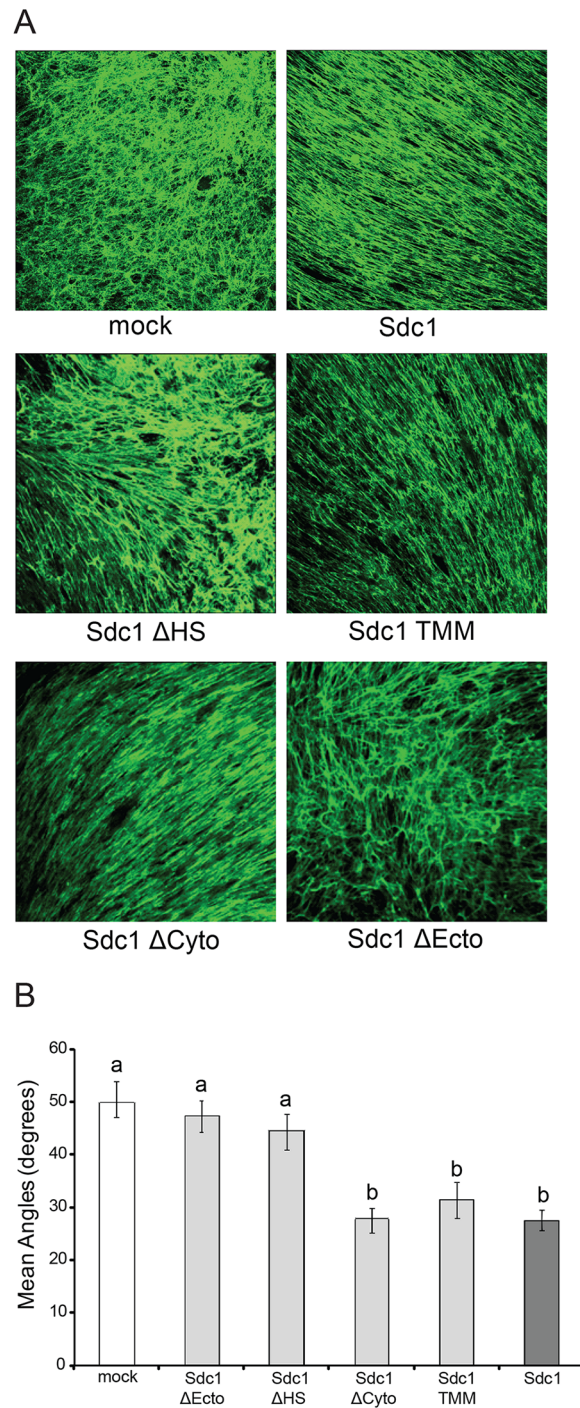
doi:10.1371/journal.pone.0150132.g001

A

B

Fig 2. Sdc1 ectodomain and HS chains are required for full activity in regulating ECM fiber alignment.
A) Representative confocal microscopy images of cell-free 3D ECMs derived from mock transfected HMF cells (mock), HMF cells expressing wildtype (Sdc1) or mutant Sdc1 (Sdc1-ΔHS, Sdc1-TMM, Sdc1-ΔCyto and Sdc1-ΔEcto). Fibronectin (FN) (green signal) in the ECMs was antibody-labeled and detected by confocal microscopy (Original magnification: 200x). B) Mean fiber-to-fiber angles of HMF-derived ECMs as indicated. ECM fiber angles were measured as described in Materials and Methods. More than 200 fiber-to-fiber angles were quantified for each Sdc1 mutant. Letters above the columns indicate the results of statistical comparisons by ANOVA. Columns sharing the same letter are not significantly different; columns labeled with different letters are significantly different (p<0.001).
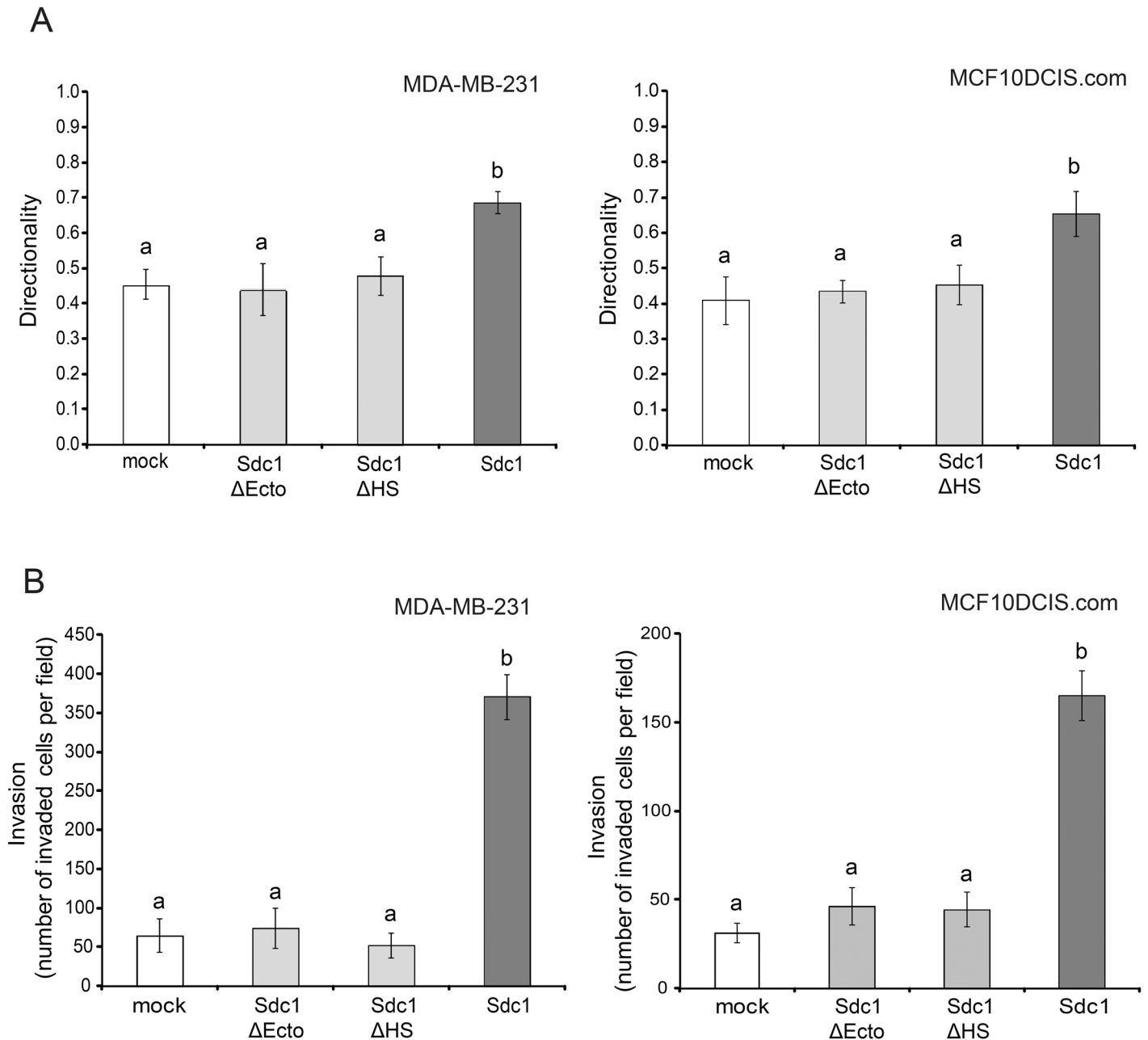
doi:10.1371/journal.pone.0150132.g002

Fig 3. Sdc1 ectodomain and HS chains are required for producing an ECM that promotes directional migration and invasion. A) Time-lapse migration study of MDA-MB-231 and MCF10DCIS.com cells in 3D ECMs derived from HMF-mock cells, HMF-Sdc1 cells, HMF cells expressing the HS-deficient Sdc1 (Sdc1-ΔHS) and HMF cells expressing the ectodomain-truncated Sdc1 (Sdc1-ΔEcto). Cell movements were recorded every 30 minutes for a period of 5–6 hours. The directional persistence of cell migration was determined as the ratio of the migration distance (net distance in a direct line from start to end point) to the total distance traveled. Columns labeled with different letters are significantly different (p<0.001). B) Invasion of MDA-MB-231 and MCF10DCIS.com cells through the indicated HMF-derived ECMs deposited in the inserts of Matrigel invasion chambers. Invasion is reported as the number of invading cells per field. Columns labeled with different letters are significantly different (p<0.001).

doi:10.1371/journal.pone.0150132.g003

with a transwell chamber-based assay. Compared to ECM-mock, a significantly greater number of cancer cells invaded through ECM-Sdc1 (Fig 3B). However, ECM-Sdc1-ΔEcto and ECM-Sdc1-ΔHS were less invasion-permissive than ECM-Sdc1 and indistinguishable from ECM-mock. These results further confirm that the HS chains and the ectodomain of Sdc1 are

required for the production of an ECM that promotes persistent directional migration and invasion of carcinoma cells and thus would be expected to stimulate tumor progression.

Integrin αvβ3 activity is required for Sdc1-mediated ECM fiber alignment

It has been shown that Sdc1 regulates the activities of several integrins, including αvβ3, αvβ5 and α2β1, via its ectodomain [32–36]. Since certain integrins play crucial roles in the initiation of FN fibrillogenesis [37–39]—a critical event in ECM assembly—we examined the possibility that Sdc1 regulates ECM fiber alignment by activating integrin ECM adhesion receptors.

As a first step towards this goal, we characterized the integrin subunit repertoire of HMF by Western blot analysis, which revealed expression of subunits α4, α5, αv, β1 and β3, whereas β4, β5 and β6 were undetectable (Fig 4A and S1 Fig). The presence of these subunits suggests that HMF carry integrins α4β1, α5β1, αvβ1 and αvβ3 on the cell surface. Among the integrins expressed by HMF, integrin αvβ3 is known to be activated by Sdc1 and to interact with the Sdc1 core protein via an integrin engagement site located within a 34–amino acid stretch of the Sdc1 ectodomain between residues 88 and 121 [31,32]–the core protein domain required for ECM fiber alignment in our model. Additionally, it has been reported that integrin αvβ3 has the ability to initiate and catalyze FN fibrillogenesis once properly activated [40,41]. Therefore, we explored the role of αvβ3 in Sdc1-mediated ECM alignment.

To suppress αvβ3 integrin activity, we silenced β3 subunit expression by siRNA. The β3 subunit forms heterodimers only with αv and αIIb subunits [42]. Since the expression of αIIb is restricted to platelets and megakaryocytes, expression silencing of the β3 subunit in HMF will only affect integrin αvβ3 activity. Western blot analysis showed that after treatment with siRNAs, the expression of the β3 subunit target was almost completely abolished in HMF mock and HMF Sdc1 cells (Fig 4B). Time course experiments revealed that a single transfection with β3 siRNAs (125nM) achieved efficient gene silencing that lasted as long as 7 days post-transfection (S2 Fig). Down-regulation of integrin αvβ3 activity in HMF Sdc1 cells diminished ECM fiber alignment in ECM-Sdc1 (Fig 4C). The mean fiber-to-fiber angles in ECMs produced by β3 siRNAs-treated HMF Sdc1 cells (ECM-Sdc1-β3 siRNAs) were significantly larger than those in ECM produced by control siRNA-treated HMF Sdc1 cells (ECM-Sdc1-control siRNA) (Fig 4D). In contrast, β3 knockdown in HMF mock had no effect on the topography of ECM produced by these cells. Similar results were obtained when αvβ3 activity was inhibited with a function-blocking antibody. Treatment of HMF Sdc1 cells with anti-αvβ3 antibody LM609 during the ECM production phase significantly reduced the FN fiber alignment (Fig 4E and 4F). The ECMs produced by HMF Sdc1 cells treated with either β3 siRNA or LM609 were somewhat more organized than ECM produced by HMF mock cells, which might be due to the functions of Sdc1 independent of αvβ3 activation or incomplete suppression of integrin αvβ3 activity by either approach. However, these results indicate that integrin αvβ3 activity is required for full Sdc1-induced ECM alignment.

The functional properties of these ECMs with respect to breast carcinoma migration and invasion were consistent with the ECM fiber angle measurements. Breast carcinoma cells seeded into ECMs derived from HMF-Sdc1, which had been treated with β3 siRNA, migrated with limited directional persistence, which was indistinguishable from carcinoma cell migration in ECM-mock (Fig 5A). Consistent with these migration results, β3 siRNA treatment of HMF-Sdc1 resulted in the production of an ECM that had lost its permissiveness to the invasion of breast carcinoma cells (Fig 5B). The migration and invasion behavior of MCF10DCIS. com cells, a model of ductal carcinoma in situ (DCIS) [43], in these ECMs was very similar to MDA-MB-231 cells (Fig 5A and 5B), indicating that the functional ECM properties are relevant not only to one migratory cell line.
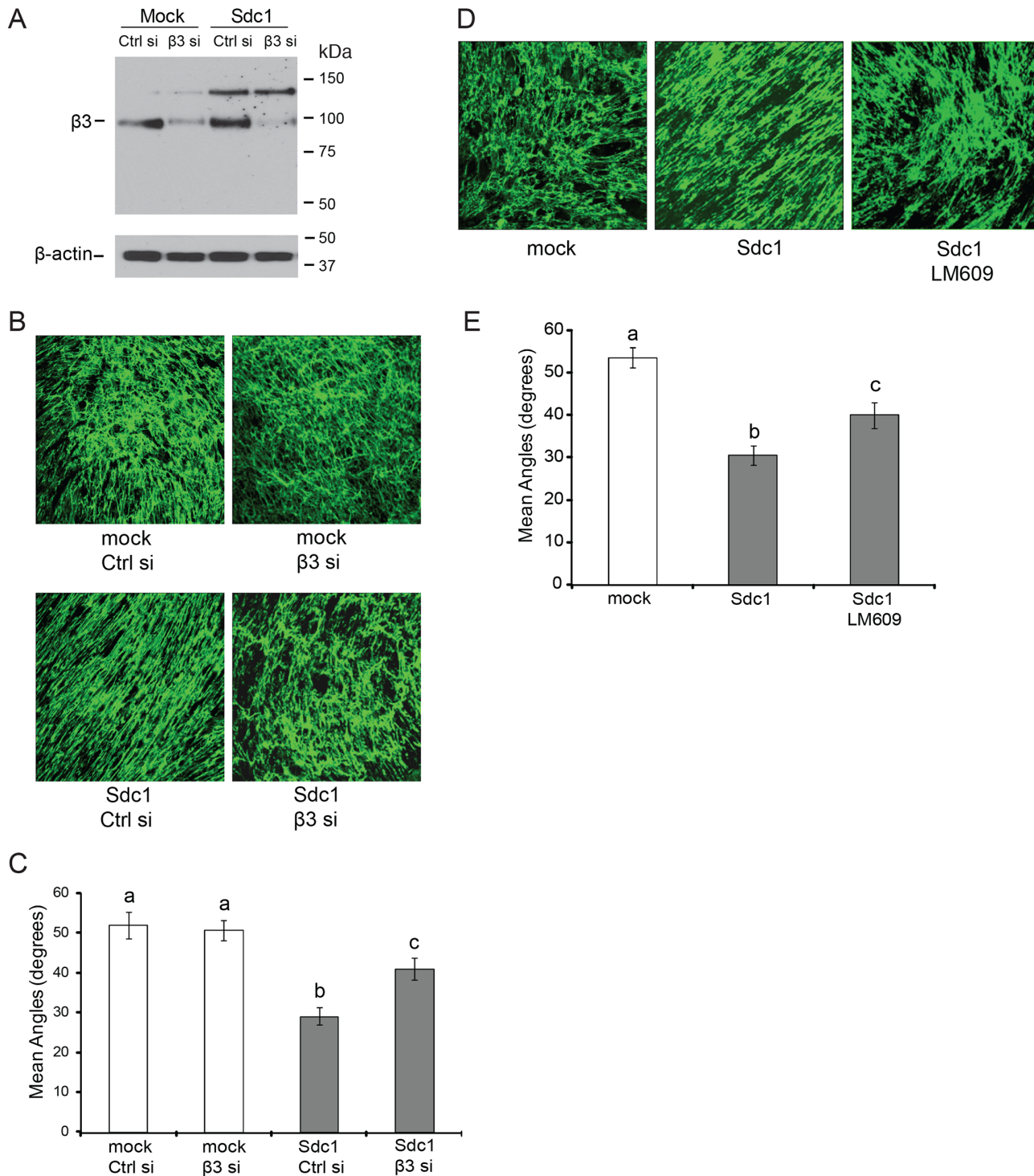
Fig 4. Integrin αvβ3 activity is required for Sdc1-mediated ECM fiber alignment. A-C) Silencing the expression of the integrin β3 subunit by siRNA diminishes ECM fiber alignment induced by Sdc1. A) Western blot analysis of integrin β3 subunit in HMF mock and HMF Sdc1 cells after treatment with control or β3 siRNA (125nM) for 3 days. B) Representative confocal microscopy images of ECMs labeled with an antibody to fibronectin (FN). The ECMs were derived from HMF-mock or HMF-Sdc1 cells treated with control or β3 siRNA. Original magnification: 200x. C) Mean fiber-to-fiber angles of ECMs produced by HMFs as indicated. Columns labeled with different letters are significantly different (at least p<0.01). D-E) Inhibition of integrin αvβ3 activity in HMF Sdc1 cells by function-blocking antibody LM609 significantly reduces FN fiber alignment. D) Representative confocal images of ECMs labeled with an antibody to FN. The ECMs were produced by HMF-mock, HMF-Sdc1 and HMF-Sdc1 treated with LM609 (30µg/ml). E) Mean fiber-to-fiber angles of HMF-derived ECMs as indicated. Columns labeled with different letters are significantly different (at least p<0.01). Ctrl si, control siRNA; β3 si, β3 siRNA.

To test the specificity of αvβ3 integrin activity in determining ECM architecture and function, we examined the role of α4β1, another integrin present in HMF with FN binding activity and purported ability to participate in ECM fibrillogenesis [44]. Knockdown of the α4 subunit, and thus disruption of α4β1 activity, had no effect on Sdc1-dependent ECM fiber alignment, suggesting that αvβ3 indeed is specifically required to mediate the Sdc1 activity (S3 Fig).
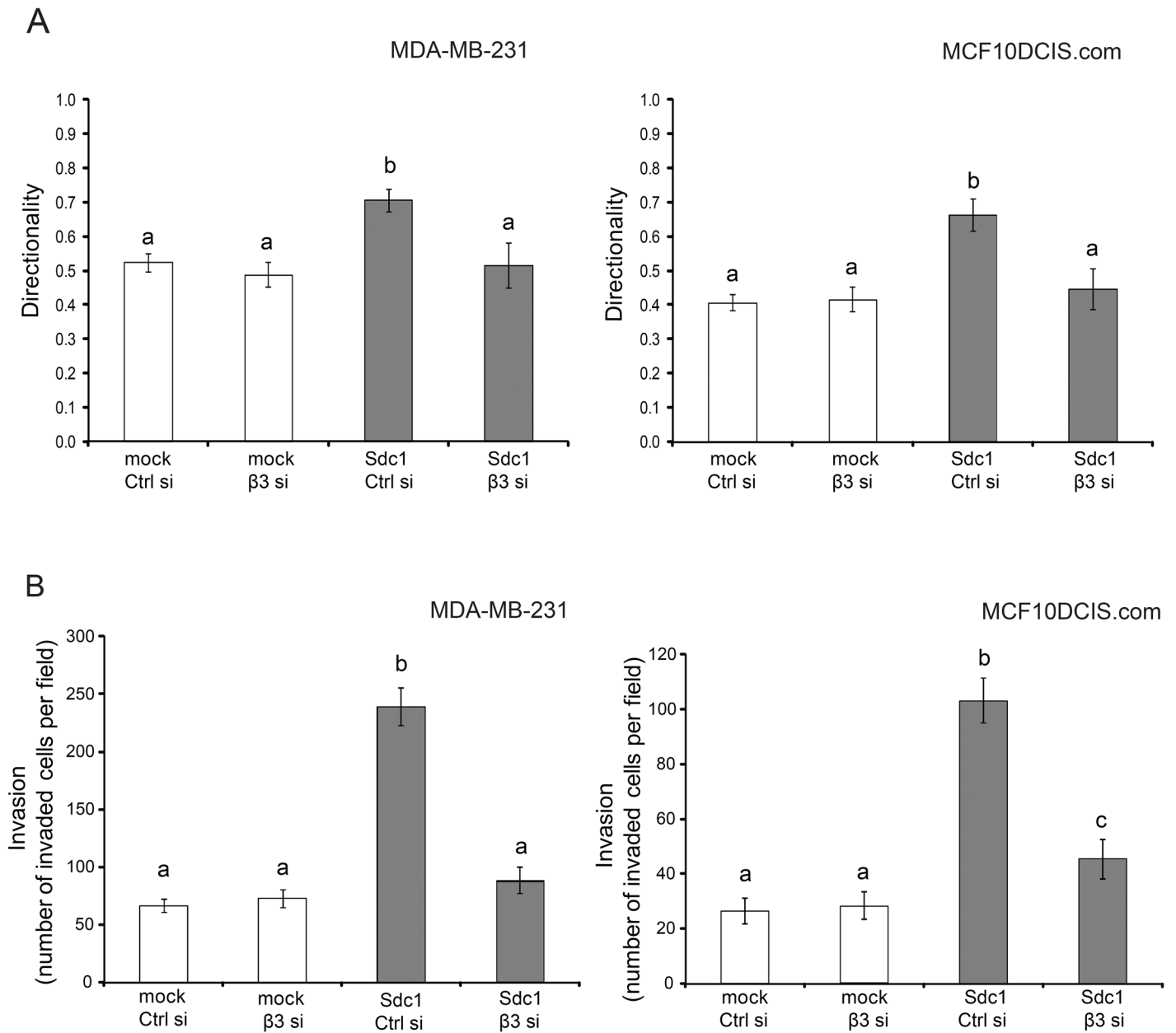

Fig 5. Silencing integrin β3 expression diminishes migration and invasion-modulating properties of the HMF-Sdc1-derived ECM. A) Quantitative assessment of migration directionality of MDA-MB-231 and MCF10DCIS.com cells within the ECMs produced by HMF-mock or HMF-Sdc1 cells treated with control or β3 siRNA using time-lapse microscopy. Different letters above columns indicate significant difference (p<0.001). B) Invasion of MDA-MB-231 and MCF10DCIS.com cells through ECMs produced by HMF-mock or HMF-Sdc1 cells treated with control or β3 siRNA. Different letters above columns indicate significant difference (at least p<0.05). Ctrl si, control siRNA; β3 si, β3 siRNA.

Integrin αvβ3 activity alone appears not to be sufficient for the generation of a fully migration and invasion-permissive ECM

To better understand the role of integrin αvβ3 in the generation of ECMs with tumor promoting properties, we tested whether the forced activation of αvβ3 would bypass the requirement for Sdc1. We chose to activate the integrin by treatment with β3 clasp peptide, an 8 amino acid peptide segment derived from the clasp region of the β3 subunit [45]. Integrins can switch between a low affinity and a high affinity conformation for ligand binding and it has been shown that the interaction between the clasp regions of the αv and β3 subunit locks the integrin αvβ3 in the low-affinity or inactive conformation. β3 clasp peptide disrupts this interaction and promotes the activation of the heterodimer [45]. To confirm the activating effect of the clasp peptide in HMF cells, a 15-minute attachment assay was performed. HMF Sdc1 cells attached more readily to surfaces coated with vitronectin (a αvβ3 substrate) than HMF mock cells (Fig 6A), indicating increased integrin αvβ3 activity in HMF Sdc1 cells. Exposure of HMF mock cells to the divalent cation Mg^{2+}, a non-specific integrin activator, stimulated attachment to a level indistinguishable from HMF Sdc1. Treatment of HMF mock cells with β3 clasp peptide dramatically enhanced cell attachment to vitronectin, to a value that was comparable to HMF Sdc1 cells. In contrast, β3 clasp peptide treatment failed to further promote the attachment of the HMF Sdc1 cells, indicating that there was no additional activation of integrin αvβ3 in these cells. Scrambled control peptides had no effect on either cell type. We concluded from these attachment assay results that the β3 clasp peptide effectively activated integrin αvβ3 in HMF mock cells.

Activation of integrin αvβ3 in HMF mock cells by treatment with β3 clasp peptide (250μM) induced changes in the ECM architecture (Fig 6B and 6C). The mean fiber-to-fiber angle in ECMs produced by β3 clasp peptide-treated HMF mock cells was more acute than in ECMs produced by control peptide-treated HMF mock cells. However, compared to the ECMs produced by HMF Sdc1 cells treated with control peptide or β3 clasp peptide, the arrangement of the FN fibers was less aligned in ECMs derived from HMF-mock, treated with β3 clasp peptide.

Invasion of MCF10DCIS.com cells through ECMs produced by β3 clasp peptide-treated HMF-mock was significantly increased compared to control-peptide-treated cells. However, β3 clasp peptide treatment of HMF failed to significantly enhance migration directionality of either MDA-MB-231 or MCF10DCIS.com cells or invasion of MDA-MB-231 cells (Fig 7A and 7B). Increasing the concentration of β3 clasp peptide to 500μM failed to further stimulate the invasion of breast carcinoma cells (N.Y., unpublished data). These results suggest that integrin αvβ3 activity is required but not sufficient for the generation of an ECM that permits directionally persistent migration and invasion of breast carcinoma cells. However, we can not entirely exclude the possibility that the clasp peptide induces suboptimal αvβ3 activation under the conditions permissive for ECM production.

Integrin αvβ3 activity is involved in Sdc1-induced elongation of HMF cells when cultured in an overconfluent state during ECM production

Cell morphology and orientation may affect ECM architecture. Syndecans play important roles in regulating cell morphology [29,46–48]. In addition, engagement of integrins may lead to actin cytoskeleton remodeling and alteration of cell morphology (for a review see [49]). Therefore, we examined and compared the morphology of HMF mock cells and HMF Sdc1 cells. HMF Sdc1 cells were morphologically indistinguishable from HMF mock when the cells were cultured on traditional two dimensional (2-D) substrate under a semiconfluent state (Fig 8A). The elongation indices of the HMF mock and HMF Sdc1 cells (ratio of cell length/width) were
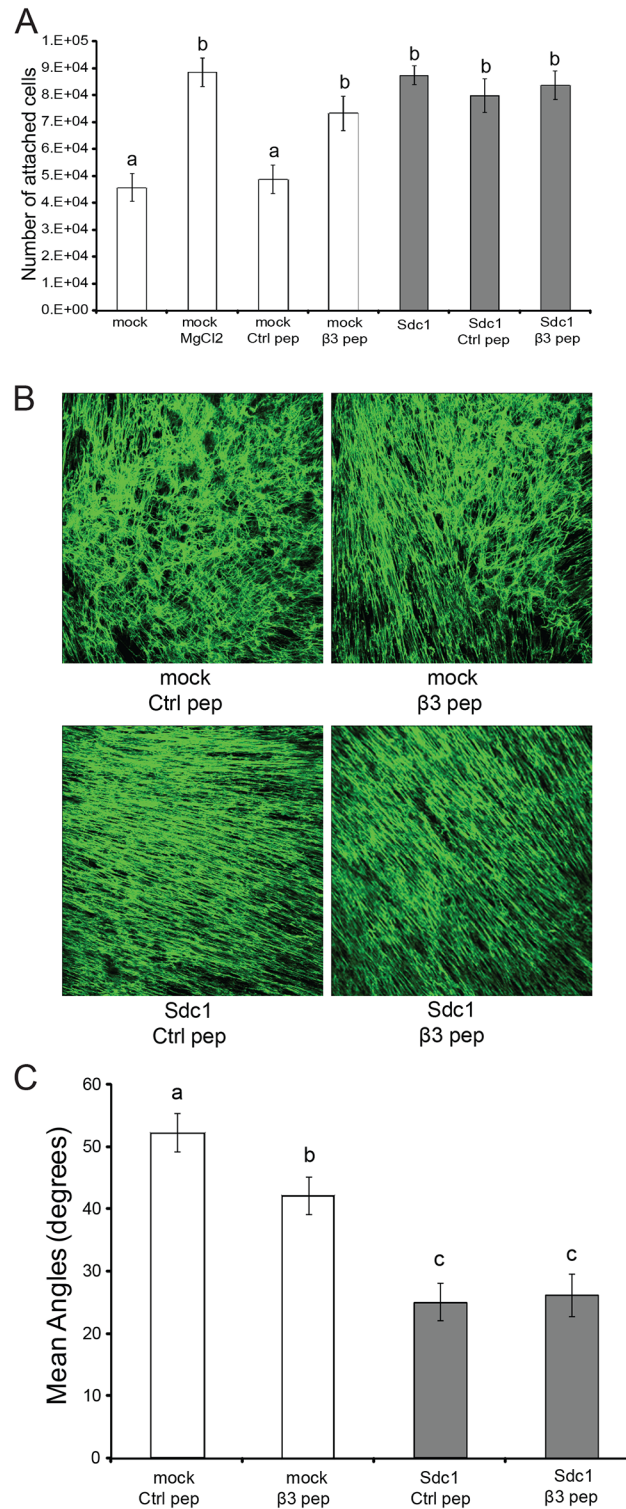
Fig 6. **Forced activation of integrin αvβ3 leads to partial ECM fiber alignment.** A) Activation of the αvβ3 integrin can be achieved independent of Sdc1 by β3 clasp peptide. Integrin αvβ3 activities were accessed by measuring the attachment of HMF cells, including untreated HMF cells, HMF cells treated with 250μM control peptide (ctrl pep), HMF cells treated with 250μM β3 clasp peptide (β3 pep) and HMF mock cells treated with 2 mM $MgCl_2$, to culture dishes pre-coated with vitronectin after 15min incubation at 37°C. Columns labeled with different letters are significantly different (at least $p < 0.05$). B) Representative confocal images of

immunofluorescently labeled FN fibers of ECMs from HMF mock and Sdc1 cells treated with control or β3 clasp peptide. Original magnification: 200x. C) Mean fiber-to-fiber angles of the indicated HMF ECMs. Columns labeled with different letters are significantly different (at least p<0.05). Ctrl pep, control peptide; β3 pep, β3 clasp peptide.
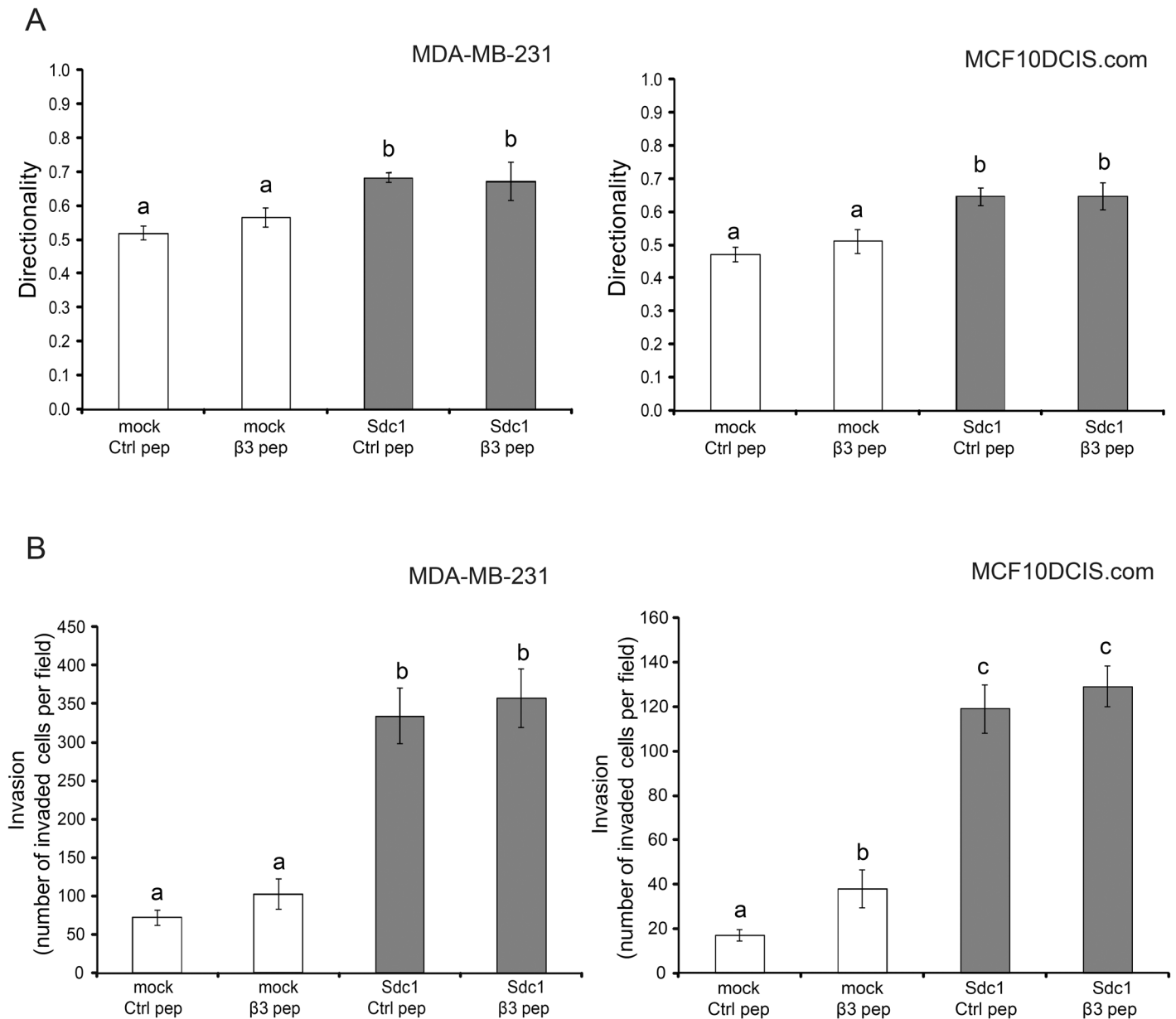
Fig 7. Activation of integrin αvβ3 alone is not sufficient for generating a migration and invasion-permissive ECM. A) Quantitative assessment of migration directionality of MDA-MB-231 and MCF10DCIS.com cells within the ECMs from HMF mock and Sdc1 cells treated with control or β3 clasp peptide using time-lapse microscopy. Columns labeled with different letters are significantly different (p<0.001). B) Invasion of MDA-MB-231 and MCF10DCIS.com cells through ECMs from HMF mock and Sdc1 cells treated with control or β3 clasp peptide. Columns labeled with different letters are significantly different (at least p<0.05). Ctrl pep, control peptide; β3 pep, β3 clasp peptide.
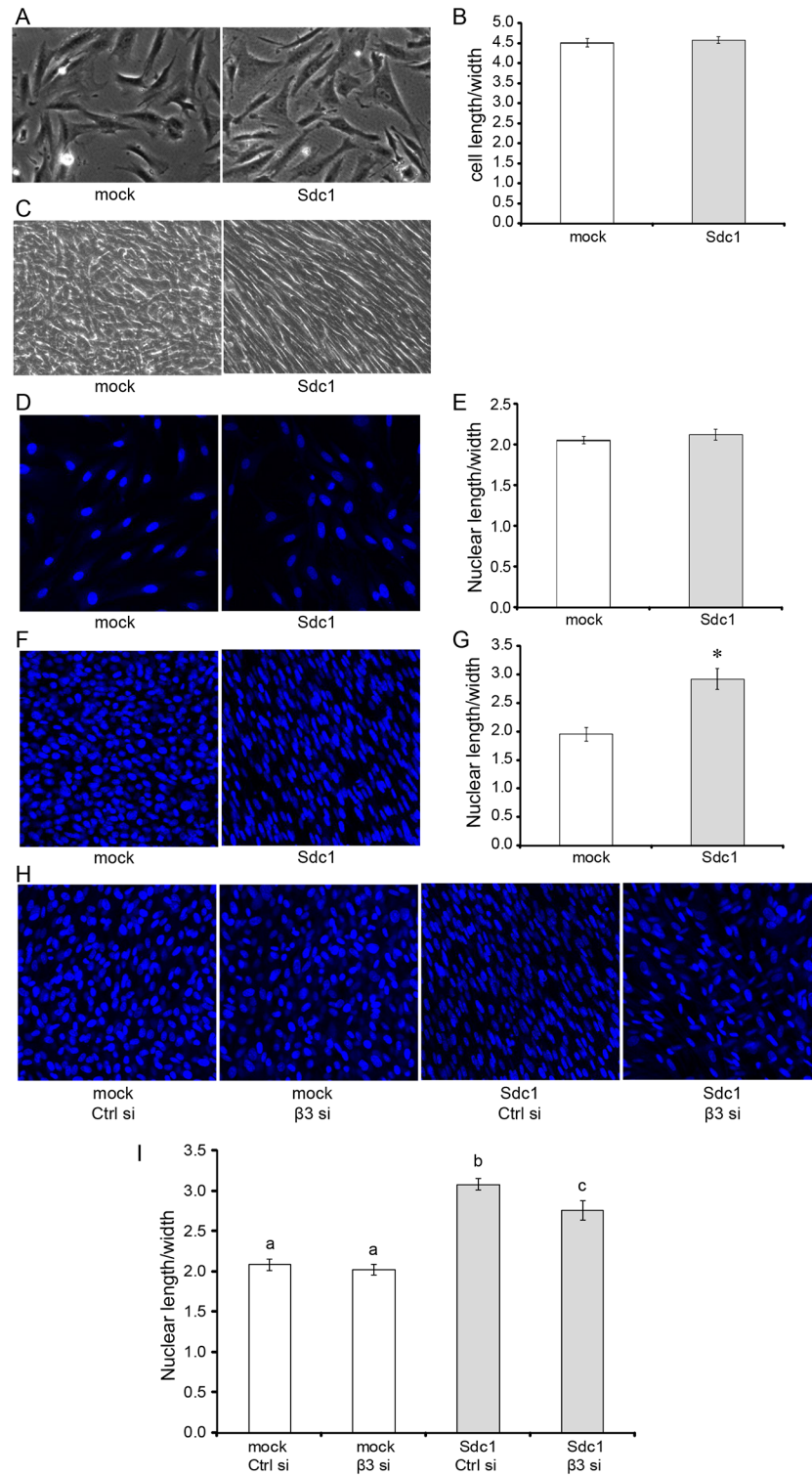
Fig 8. Integrin αvβ3 activity is involved in Sdc1-induced morphological changes during 3D ECM production. A-B, representative phase contrast images of HMF mock and Sdc1 cells cultured on gelatin-coated plates under semiconfluent states (A; original magnification: 100x) and the corresponding mean elongation indices (ratio of cell length/width) of HMF mock and Sdc1 cells (B). C, representative phase contrast images of HMF mock and Sdc1 cells after 7 d of culture under conditions permissive for 3D ECM production (Original magnification: 100x). D-E, representative confocal images of the nuclei of HMF mock

and Sdc1 cells cultured on gelatin-coated plates under semiconfluent states (D; original magnification: 200x) and the corresponding mean nuclear elongation indices (ratio of nuclear length/width) of HMF mock and Sdc1 cells (E). The nuclei were labeled with Hoechst 33342. F-G, representative confocal images of the nuclei of HMF mock and Sdc1 cells after 7 d of culture under conditions permissive for 3D ECM production (F; Original magnification: 200x) and the corresponding mean nuclear elongation indices of HMF mock and Sdc1 cells (G). The nuclei were labeled with Hoechst 33342. *indicates that the difference was statistically significant (p<0.0001). H-I, representative confocal images of the nuclei of control siRNA or β3 siRNA treated HMF mock and Sdc1 cells after 7 d of culture under conditions permissive for 3D ECM production (H; original magnification: 200x) and the corresponding mean nuclear elongation indices (I). SiRNA treatment was performed as described in Material and Methods. The nuclei were labeled with Hoechst 33342. Letters above the columns indicate the results of statistical comparisons by ANOVA. Columns sharing the same letter are not significantly different; columns labeled with different letters are significantly different (at least p<0.05).

virtually identical (Fig 8B). However, clear morphological differences were detected between HMF mock and Sdc1 cells when the cells were cultured in an overconfluent state under the condition permissive for ECM production. Phase contrast images of ECM cultures of HMF cells showed that while HMF mock cells exhibited a more rounded cell shape, Sdc1-overexpressing HMF Sdc1 cells became much more elongated and gained a spindle-shaped morphology (Fig 8C). The morphological changes of HMF Sdc1 occurred early during ECM production. HMF Sdc1 became spindle-shaped after 2 days of culture under the conditions required to produce 3-D ECM (data not shown). We attempted to analyze the morphological changes of HMF Sdc1 cells quantitatively. However, HMF cells formed multiple layers during the 7 days of culture, making it impossible to clearly outline cell contours and therefore to determine elongation indices [50,51]. It has been shown that cell shape is positively correlated with nuclear shape [50,51]. Therefore, we compared the nuclear shape and nuclear elongation indices (nuclear length/width) of HMF cells. Indeed, we found that there were no significant differences in nuclear shape and nuclear elongation indices between HMF mock and Sdc1 cells when the cells were cultured on 2-D substrate in a semiconfluent state (Fig 8D and 8E). However, the nuclei of HMF Sdc1 cells became greatly elongated after 7 days of culture under conditions permissive for ECM production (Fig 8F). The nuclear elongation index of HMF Sdc1 cells was markedly increased and became significantly larger compared to the nuclear elongation index of HMF mock cells (Fig 8G). Moreover, knockdown of the expression of integrin β3 subunit by siRNA in Sdc1-overexrpessing HMF Sdc1 cells resulted in a less elongated nuclear morphology when the cells were cultured in an overconfluent state under the conditions permissive for ECM production (Fig 8H). The nuclear elongation index of HMF SDC1 cells treated with siRNA against integrin β3 subunit was significantly decreased in comparison to HMF Sdc1 cells treated with control siRNA (Fig 8I). The results suggest that Sdc1 overexpression induces morphological changes in HMF cells through αvβ3 integrin, which may account for one of the mechanisms by which Sdc1 mediates ECM fiber alignment.

Discussion

A growing body of evidence indicates that composition and physical properties of the ECM are altered in breast cancer and that these changes contribute to cancer progression [7,8,13,52]. Much of this work has focused on ECM density and rigidity [7,13,53] but more recently, ECM fiber alignment also has been shown to predict invasion and metastasis [11,25,54]. The Cukierman group reported that murine skin tumor fibroblasts produce an ECM with aligned, parallel fibers when cultured in 3D [55]. Work by Provenzano and colleagues demonstrated that in Wnt-1 and PyMT-induced mouse mammary tumors, collagen fibers organize progressively around the tumor islets [11]. As the tumor becomes invasive, collagen fibers become aligned and eventually orientated perpendicularly to the advancing edge of the tumor. This collagen

fiber organization, termed by the investigators "tumor-associated collagen signature-3" (TACS-3), facilitates the invasion of tumor cells into the stroma and metastasis. Moreover, the presence of TACS-3 features serves as a prognostic indicator of poor outcome in human breast cancer [54]. The Tlsty group found that transformed mammary epithelial cells or carcinoma cells assume a mesenchymal phenotype when co-cultured and metastasize more readily when co-inoculated with carcinoma-associated fibroblasts (CAF) compared to reduction mammo-plasty fibroblasts (RMF), a difference that could be attributed to the deposition of a distinct, aligned ECM [56]. The ECM architecture may also mediate the effects of pregnancy and lactation on mammary tumor development. For example, the spatial organization of fibrillar collagen, which is haphazardly arranged in glands of parous rats and more linearized/aligned in glands of nulliparous animals, is the main determinant of whether mammary ECM suppresses or promotes tumor cell invasion [57].

To date, the mechanism by which the architecture of the ECM fibers is regulated has remained largely unknown. Recently, we have identified Sdc1 as a potent regulator of ECM architecture [25]. While Sdc1 expression in stromal fibroblasts is not required for ECM production, its presence alters ECM architecture *in vivo* and *in vitro*, resulting in an aligned, parallel ECM fiber organization that promotes the directional migration and invasion of breast carcinoma cells. Other syndecan family members have also been implicated in ECM assembly. Sdc2 promotes the production of a FN matrix in CHO cells by activating various integrins [58]. Sdc4 participates in regulating FN fibrillogenesis by associating with α5β1 integrin and possibly by activating Rho and protein kinase C (PKC) [59]. In corneal stromal cells of the eye, Sdc1 is required for efficient FN fibrillogenesis but becomes dispensable when integrins are generically activated by $MnCl_2$, suggesting that the role of Sdc1 in ECM assembly involves the regulation of integrin activity [60]. Curiously, in the same study, Sdc1 deficiency resulted in increased FN fibrillogenesis in fibroblasts.

In the present study, we explored the mechanisms by which Sdc1 modulates ECM architecture. Our data show that HMF cells overexpressing Sdc1 exhibit a more elongated, spindle-shaped cell morphology when the cells were cultured in an overconfluent state under the conditions permissive for ECM production, which is significantly different from the morphology of mock transfected HMF cells. Similar morphological differences have been observed between cultures of tumor-associated fibroblasts and normal fibroblasts, which produce aligned ECM and randomly organized ECM respectively [55]. In addition, FAP+ fibroblasts that organize ECM fibers in parallel patterns are also found to become elongated into an enhanced spindled shape [61]. Goetz et al observed that caveolin-1, a caveolar scaffolding protein, is required for fibroblast elongation, efficient ECM fiber alignment and the elongation of cells seeded into these matrices [62].

Cell morphology and orientation affects ECM architecture. We have shown previously that mammary fibroblasts, which are forced to elongate and align by plating them on patterned FN surfaces, produce an ECM with an aligned fiber architecture [25]. Therefore, it is likely that the altered cell morphology induced by Sdc1 plays a role in the production of an aligned ECM. Sdc1 directly interacts with and activates the integrin αvβ3 via its ectodomain [32,63]. It is well known that engagement of integrins may lead to the remodeling of the actin cytoskeleton and an alteration of cell shape (for a review see [64]). Therefore, Sdc1 may modulate cell morphology though activating integrin αvβ3, thereby altering ECM architecture. Our findings that downregulation of the expression of integrin β3 subunit by siRNA in Sdc1-overexpressing HMF cells leads to a less elongated cell morphology and more random ECM organization are consistent with the above hypothesis. However, we cannot exclude the possibility that the morphological change of HMF Sdc1 cells is the result rather than the cause of ECM alignment. HMF cells continue to produce ECM during the 7-day culture period. ECM topography and

composition influence cell morphology. It has been demonstrated that the aligned ECM produced by tumor associated fibroblasts is sufficient to induce a spindle-shaped morphology in normal primary fibroblasts [55].

It is also possible that Sdc1 induces ECM fiber alignment by modulating FN fibrillogenesis. FN is the major component of the provisional ECM into which other ECM components such as collagens, fibulin-1, thrombospondin-1 and tenascin-C are then integrated (reviewed in [65]). By regulating the topography of the FN-rich provisional ECM, Sdc1 may govern the architecture and function of the mature fibroblast-derived ECM. FN fibrillogenesis is a complex, cell-driven process in which cell surface receptors such as integrins and HSPGs play essential roles. FN is composed of three types of repeating modules, which include 12 type I repeats, 2 type II repeats, and 15 type III repeats. FN is secreted as compactly folded, disulfide-bonded dimers that are functionally inactive. Binding of FN dimers to integrins at the cell surface triggers a series of cellular events, eventually resulting in conformational changes in FN that unravel the cryptic FN self-association sites and convert the molecule into an extended and active form (for reviews, see [65–67]). The requirement of Sdc1 HS chains and integrin αvβ3 in our experiments suggests that stromal Sdc1 may modulate FN fibrillogenesis by both direct and indirect mechanisms. Two high affinity heparin binding domains, Hep I and Hep II, have been identified in FN, which interact with the HS chains of various members of the syndecan family [68,69]. Hep I and Hep II domains map to the type I_{1-5} and type III_{12-14} repeats, respectively [70]. It has been shown that the type I_{1-5} repeats also harbor a major site for FN self-assembly and the type III_{12-14} repeats are essential for the intramolecular interactions that maintain the compact, globular conformation of FN dimers [71,72]. Once expressed by stromal fibroblasts, Sdc1 may in part directly regulate the unfolding of dimeric FNs and the interactions between cell-associated FN dimers through its HS chains, thus affecting the architecture of the multimeric FN fibrils.

Sdc1 directly interacts with and activates the integrin αvβ3 via its ectodomain [32,63]. While the assembly of FN fibril matrix appears to be initiated mainly by integrin α5β1 [37,73], integrin αvβ3 also has the ability to support this process once properly activated [40,41,74]. Integrin α5β1 and αvβ3 differ in their requirements for binding sites on FN. Integrin α5β1 requires a synergy region located in type III_9 repeats in addition to the Arg-Gly-Asp (RGD) motif for obtaining maximal binding to FN, whereas αvβ3 utilizes a binding site located in N-terminal type I_{1-5} repeats besides the RGD motif [75–78]. Moreover, there is evidence that FN fibrils generated by αvβ3 integrin activity display distinct features from those produced by α5β1 [40,74]. It is possible that in Sdc1-negative fibroblasts, α5β1 functions as the major integrin for the initiation of FN fibrillogenesis, forming an intricate meshwork of FN fibrils. In fibroblasts overexpressing Sdc1, the activity of integrin αvβ3 is greatly increased. The initiation of FN fibrillogenesis in Sdc1-overexpressing fibroblasts may be conducted mainly by integrin αvβ3, which, in combination with the effects of HS chains of Sdc1, results in the production of an aligned ECM that is different from the ECM assembled under the control of α5β1. In this context, it is interesting that the stromal ECM of carcinomas growing in β3 integrin deficient mice contains thicker, laterally fused collagen fibers, contrasting with the delicate fibers seen in wild-type animals [79]. How these findings relate to the Sdc1-dependent fiber alignment is uncertain but they are congruent with our data by demonstrating a dramatic effect of β3 integrin activity on ECM fiber architecture *in vivo*.

In summary, we have demonstrated a regulatory effect of Sdc1 on the tumor ECM architecture. Sdc1 is aberrantly expressed in stromal fibroblasts of invasive breast carcinomas, leading to an aligned ECM fiber architecture. Our data suggest that multiple mechanisms may contribute to Sdc1-induced ECM alignment. Sdc1 expression alters the morphology of fibroblasts through integrin αvβ3. In addition, Sdc1 may modulate the assembly of 3D fibrillar ECM by

directly interacting with FN via its HS chains and by activating integrin αvβ3 via its ectodomain (shown schematically in Fig 9). These ECM remodeling events convert the stroma from an invasion-restrictive to an invasion-permissive microenvironment and create "highways" that may facilitate the invasion and spreading of breast carcinoma cells.

Materials and Methods

Cell culture

Immortalized human mammary fibroblasts were kindly provided by Dr. C. Kuperwasser [80]. The human breast carcinoma cell lines MDA-MB-231 and MCF10DCIS.com [43] were purchased from ATCC (Manassas, VA) and Asterand (Detroit, MI), respectively. Stable cell lines derived from HMF that expressed wildtype and mutant forms of Sdc1 or empty plasmid were maintained in DMEM supplemented with 10% calf serum, 2 mM L-glutamine, 100U/mL penicillin/streptomycin and 250 µg/ml G418. MDA-MB-231 cells were cultured in DMEM supplemented with 10% fetal bovine serum, 2 mM L-glutamine and 100U/mL penicillin/streptomycin. MCF10DCIS.com cells were maintained in DMEM/F12 medium containing 5% horse serum and 100U/mL penicillin/streptomycin.

Stable transfections

The generation of mock-transfected HMF and HMF stably transfected with Sdc1 has been described previously [25]. Mammalian expression vectors (pcDNA3.1) containing the cDNAs encoding truncated and mutated mouse Sdc1 were generous gifts from Dr. Ralph Sanderson (University of Alabama, Birmingham) and Dr. Alan Rapraeger (University of Wisconsin-Madison, Madison, WI). The Sdc1 mutant constructs included a heparan sulfate-deficient mutant (Sdc1-ΔHS) [28], an ectodomain truncation mutant (Sdc1-ΔEcto) [32], a transmembrane domain substitution mutant (Sdc1-TMM) [29] and a cytoplasmic domain deletion mutant (Sdc1-ΔCyto) [30]. The syndecan-1 mutant constructs were stably transfected into HMF cells using the Amaxa System (Lonza, USA) according to the manufacturer's instructions. Following transfection, cells were selected with 500 g/ml G418 and cells that expressed mutant Sdc1 at levels similar to wild-type Sdc1 were enriched by fluorescence-activated cell sorting (FACS).

3D ECM production

Preparation of the HMF-derived, *in vivo*-like ECM was performed according to the protocol developed by Cukierman and has been described previously [25,55,81]. Briefly, HMF cells were cultured in a highly confluent state for 7 days in the presence of 50 µg/ml sodium ascorbate (Fisher Scientific, Inc., Pittsburgh, PA) and then removed by alkaline detergent treatment (25 mM Tris-HCl, pH 7.4, 150 mM NaCl, 0.5% Triton X-100, and 20 mM NH_4OH), leaving a cell-free 3D ECM attached to the culture surface.

Analysis of ECM fiber orientation/alignment

The architecture of HMF-derived ECMs was visualized by immunofluorescence staining of the fibronectin (FN) fibers. The cell-free 3D ECMs were blocked with 5% FBS for 1 h at room temperature and then incubated with mouse anti-FN (BD Biosciences, San Juan, CA) antibody at 4°C overnight. After incubation with Alexa Fluor488 conjugated goat anti-mouse IgG for 1 h at room temperature, the ECM preparations were imaged with a laser-scanning confocal microscope. As previously described, the fiber-to-fiber angles of the ECMs were determined manually by overlaying the ECM images with a pre-designed template that defined nine evenly
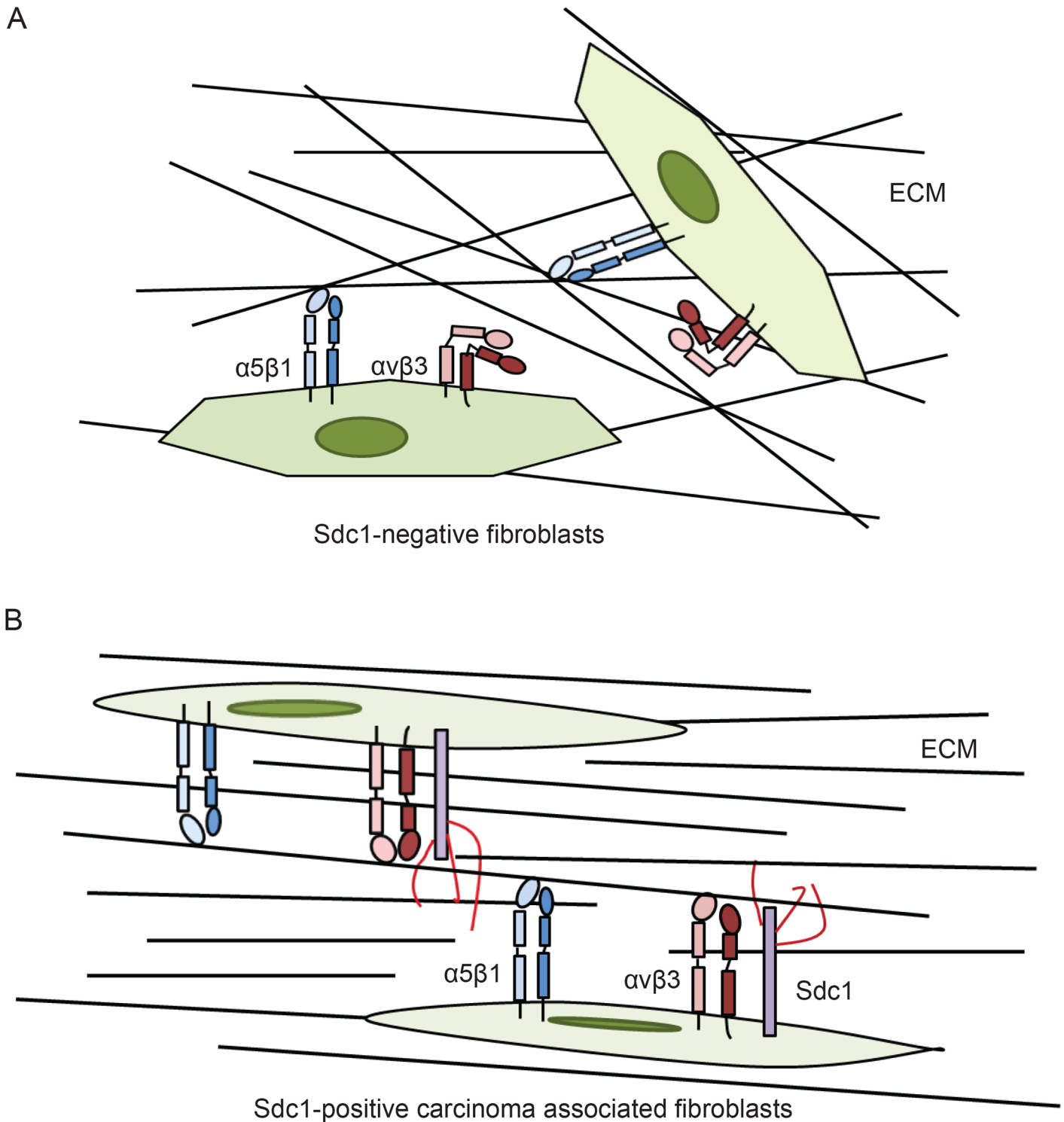
Fig 9. Potential molecular mechanisms by which stromal Sdc1 regulates ECM fiber alignment. A) In Sdc1-negative normal fibroblasts, FN fibrillogenesis is likely initiated by integrin α5β1, which gives rise to an ECM with haphazard fiber arrangement. B) In the stromal fibroblasts of some invasive breast carcinomas, Sdc1 is aberrantly expressed. Sdc1 induces morphological changes of the fibroblasts, which may contribute to the production of aligned ECM. Sdc1 may also modulate FN fibrillogenesis by directly regulating the unfolding of dimeric FNs and the interactions between cell-associated FN dimers through its HS chains. In addition, Sdc1 may modulate the initiation of FN fibrillogenesis by activating integrin αvβ3 through its ectodomain. The combined effects of Sdc1 affect the architecture of the multimeric FN fibrils, resulting in an ECM with an organized, aligned fiber arrangement.

doi:10.1371/journal.pone.0150132.g009

distributed measurement points. The fiber closest to each of the measurement points was identified and the intersection angle of the nearest crossing fiber was measured using the angle measurement tool of ImageJ (http://rsbweb.nih.gov/ij/) [25]. At least 90 fiber-to-fiber angles were measure for each condition/group.

siRNA transfections

Knockdown of integrins was achieved by using the ON-TARGET*plus* SMARTpool siRNAs (Thermo Scientific, Rockford, IL). The ON-TARGETplus Non-targeting Pool served as negative controls. Transfection of the siRNAs was performed using Dharmafect 3 transfection reagent according to the manufacturer's instructions (Thermo Scientific). Briefly, semiconfluent HMF cells were incubated with the transfection mixture containing 100-125nM of siRNAs for 72 hr. Cells were then harvested for Western blot analysis to confirm the knockdown of integrin expression and for the production of the 3D ECMs.

Western blot analysis

Whole cell lysates of HMF cells were prepared using RIPA buffer (Boston BioProducts). Equal amounts of the resulting protein lysates were fractionated on 4–12% Criterion™ XT precast gel (Bio-Rad Laboratories, Inc) prior to transfer to polyvinylidene difluoride (PVDF) membranes. The membranes were probed with rabbit anti-human integrin α4 or rabbit anti-human integrin β3 antibodies (Cell Signaling Technology, Inc) at 4°C overnight, washed in 1xPBS, and then incubated with horseradish peroxidase-conjugated anti-rabbit IgGs (Sigma) at room temperature for 1 hr. The integrin α4 or integrin β3 subunit was visualized using the SuperSignal West Femto maximum sensitivity substrate (Pierce).

Integrin stimulation

β3 clasp peptide and its scrambled control were designed based on published reports by Vomund *et al.* [45] and synthesized and purified by Biomatik (Wilmington, DE). The activation of integrin αvβ3 by β3 clasp peptide was confirmed using a 15-minute cell attachment assay. HMF cells were harvested and incubated with control or β3 clasp peptide for 30 minutes. Cells were then added to culture dishes precoated with the integrin αvβ3 substrate vitronectin and incubated at 37°C for 15 minutes. The unattached cells were removed by washing with PBS and attached cells were collected and counted using a hemocytometer. To investigate the effect of integrin αvβ3 activation on the architecture of the ECM, control and β3 clasp peptide were added to the medium throughout the process of matrix production.

Cell migration analysis (time-lapse motility assay)

Live MDA-MB-231 and MCF10DCIS.com cells were fluorescently labeled using the CellBrite cytoplasmic membrane staining kit (Biotium, Inc., Hayward, CA) according to the manufacturer's instructions. Labeled cells were seeded into glass-bottom tissue culture plates (MatTek Corporation, Ashland, MA) precoated with cell-free ECMs derived from HMF cells and incubated overnight. Cell movements were recorded every 30 minutes for a period of 5–6 hours on the BD Pathway confocal bioimager (BD Biosciences). The resulting images were stacked using the ImageJ software and the movement of individual cells was monitored by tracing the path of the manually detected cell center using the Fragment Line tool of ImageJ. The directional persistence of migration was determined as the ratio of net distance between starting point and end point to the total distance traveled.

Invasion assay

HMF cells were cultured in the insert of BD Biocoat Matrigel Invasion Chambers (BD Biosciences) under conditions conducive to ECM production for 7 days. The cells were then removed to leave cell-free ECMs on the upper side of the insert. Breast carcinoma cells MDA-MB-231 or MCF10DCIS.com were seeded into these ECMs and cultured in DMEM supplemented with 2% calf serum or DMEM/F12 containing 1% horse serum for 24 hours. The lower chambers were filled with DMEM containing 10% calf serum or DMEM/F12 containing 5% horse serum as a source of chemoattractants. Non-invading carcinoma cells remaining on the upper side of the insert were removed. The invading cells attached to the lower side of the insert were fixed with 100% methanol and stained with Hoechst 33342 DNA dye. Images of the stained nuclei were acquired using an Olympus inverted microscope and analyzed using ImageJ software.

Nuclear staining

HMF cells cultured in glass-bottom dishes were fixed with ice-cold 100% methanol for 15 min. Subsequently, the cells were incubated with the cell-permeable nucleic acid stain Hoechst 33342 (20µg/ml) for 30 min. The stained nuclei of HMF cells were imaged using the Nikon A1R-Si laser scanning confocal spectral microscope.

Quantitative analysis of the morphology of HMF cells

Cellular and nuclear morphology of HMF cells were evaluated by calculating the elongation indices (length-to-width ratios) of the cells and their nuclei. HMF cells were either cultured on gelatin-coated glass-bottom plates at a semi-confluent state overnight or cultured in a highly confluent state for up to 7 days under conditions required for 3D ECM production. Phase contrast images of the HMF cells and confocal images of the Hoechst-stained HMF cells were analyzed using ImageJ software. Cell length was defined as the longest distance between any two points on the cell contour. Cell width was defined as the longest distance within the cell body perpendicular to the length. Nuclear length and width were defined as the length of the major (long) axis and minor (short) axis of the nucleus, respectively.

Statistics

All the experiments were repeated at least two times. The experimental results were presented as mean ± standard deviation and statistically analyzed using the InStat 3.1 software (Graph-Pad Software, Inc., USA). Multiple paired comparisons were conducted using one-way ANOVA followed by Tukey's post-hoc test. P values of less than 0.05 were considered statistically significant unless otherwise indicated.

Supporting Information

S1 Fig. Western blot analysis of various integrin subunits in HMF mock and HMF Sdc1 cells. HMF cells express integrin subunits α4, α5, αv, β1 and β3.
(TIF)

S2 Fig. Western blot analysis of integrin β3 subunit in HMF mock and HMF Sdc1 cells. Treatment with β3 siRNA (125 nM) successfully suppresses the expression of β3 subunit in HMF cells even 7 days after siRNA transfection.
(TIF)

S3 Fig. Silencing the expression of integrin α4 subunit has no effect on Sdc1-induced ECM fiber alignment. A, Western blot analysis of the level of integrin α4 subunit in HMF mock and

HMF Sdc1 cells after treated with 100nM control or α4 siRNA for 3 days. B, representative confocal images of immunofluorescently labeled FN fibers of ECMs from HMF mock and Sdc1 cells treated with control or α4 siRNA. Original magnification: 200x. C, mean fiber-to-fiber angles of indicated HMF ECMs. Columns labeled with different letters are significantly different (p<0.001). Ctrl si, control siRNA; α4 si, α4 siRNA.
(TIF)

Acknowledgments

Author Contributions

Conceived and designed the experiments: AF NY. Performed the experiments: NY. Analyzed the data: NY. Wrote the paper: NY AF.

References

1.   Lu P, Takai K, Weaver VM, Werb Z. Extracellular matrix degradation and remodeling in development and disease. Cold Spring Harb Perspect Biol. 2011; 3. doi: 10.1101/cshperspect.a005058

2.   Ozbek S, Balasubramanian PG, Chiquet-Ehrismann R, Tucker RP, Adams JC. The evolution of extracellular matrix. Mol Biol Cell. 2010; 21: 4300–4305. doi: 10.1091/mbc.E10-03-0251 PMID: 21160071

3.   Huijbers IJ, Iravani M, Popov S, Robertson D, Al-Sarraj S, Jones C, et al. A role for fibrillar collagen deposition and the collagen internalization receptor endo180 in glioma invasion. PloS one. 2010; 5: e9808. doi: 10.1371/journal.pone.0009808 PMID: 20339555

4.   Kauppila S, Stenbäck F, Risteli J, Jukkola A, Risteli L. Aberrant type I and type III collagen gene expression in human breast cancer in vivo. The Journal of Pathology. 1998; 186: 262–268.

5.   Barcus CE, Keely PJ, Eliceiri KW, Schuler LA. Stiff collagen matrices increase tumorigenic prolactin signaling in breast cancer cells. Journal of Biological Chemistry. American Society for Biochemistry and Molecular Biology; 2013; 288: 12722–12732. doi: 10.1074/jbc.M112.447631

6.   Beacham DA, Cukierman E. Stromagenesis: the changing face of fibroblastic microenvironments during tumor progression. Semin Cancer Biol. 2005; 15: 329–341. doi: 10.1016/j.semcancer.2005.05.003 PMID: 15970443

7.   Levental KR, Yu H, Kass L, Lakins JN, Egeblad M, Erler JT, et al. Matrix crosslinking forces tumor progression by enhancing integrin signaling. Cell. 2009; 139: 891–906. doi: 10.1016/j.cell.2009.10.027 PMID: 19931152

8.   Locker J, Segall JE. Breast cancer: the matrix is the message. Am J Pathol. 2011; 178: 966–968. doi: 10.1016/j.ajpath.2010.12.013 PMID: 21356348

9.   Parekh A, Weaver AM. Regulation of cancer invasiveness by the physical extracellular matrix environment. Cell Adh Migr. 2009; 3: 288–292. PMID: 19458499

10. Paszek MJ, Boettiger D, Weaver VM, Hammer DA. Integrin clustering is driven by mechanical resistance from the glycocalyx and the substrate. PLoS Comput Biol. 2009; 5: e1000604. doi: 10.1371/journal.pcbi.1000604 PMID: 20011123

11. Provenzano PP, Eliceiri KW, Campbell JM, Inman DR, White JG, Keely PJ. Collagen reorganization at the tumor-stromal interface facilitates local invasion. BMC Med. 2006; 4: 38. doi: 10.1186/1741-7015-4-38 PMID: 17190588

12. Salmon H, Franciszkiewicz K, Damotte D, Dieu-Nosjean M-C, Validire P, Trautmann A, et al. Matrix architecture defines the preferential localization and migration of T cells into the stroma of human lung tumors. J Clin Invest. 2012; 122: 899–910. doi: 10.1172/JCI45817 PMID: 22293174

13. Schedin P, Keely PJ. Mammary gland ECM remodeling, stiffness, and mechanosignaling in normal development and tumor progression. Cold Spring Harb Perspect Biol. 2011; 3: a003228. doi: 10.1101/cshperspect.a003228 PMID: 20980442

14. Choi Y, Chung H, Jung H, Couchman JR, Oh E-S. Syndecans as cell surface receptors: Unique structure equates with functional diversity. Matrix Biol. 2011; 30: 93–99. doi: 10.1016/j.matbio.2010.10.006 PMID: 21062643

15. Couchman JR. Transmembrane signaling proteoglycans. Annu Rev Cell Dev Biol. 2010; 26: 89–114. doi: 10.1146/annurev-cellbio-100109-104126 PMID: 20565253

16. Tkachenko E, Rhodes JM, Simons M. Syndecans: new kids on the signaling block. Circ Res. 2005; 96: 488–500. doi: 10.1161/01.RES.0000159708.71142.c8 PMID: 15774861

17. Bernfield M, Sanderson RD. Syndecan, a developmentally regulated cell surface proteoglycan that binds extracellular matrix and growth factors. Philos Trans R Soc Lond, B, Biol Sci. 1990; 327: 171–186. PMID: 1969657

18. Vainio S, Jalkanen M, Bernfield M, Saxén L. Transient expression of syndecan in mesenchymal cell aggregates of the embryonic kidney. Dev Biol. 1992; 152: 221–232. PMID: 1644217

19. Vainio S, Lehtonen E, Jalkanen M, Bernfield M, Saxén L. Epithelial-mesenchymal interactions regulate the stage-specific expression of a cell surface proteoglycan, syndecan, in the developing kidney. Dev Biol. 1989; 134: 382–391. PMID: 2663574

20. Anttonen A, Kajanti M, Heikkilä P, Jalkanen M, Joensuu H. Syndecan-1 expression has prognostic significance in head and neck carcinoma. Br J Cancer. 1999; 79: 558–564. doi: 10.1038/sj.bjc.6690088 PMID: 10027330

21. Baba F, Swartz K, van Buren R, Eickhoff J, Zhang Y, Wolberg W, et al. Syndecan-1 and syndecan-4 are overexpressed in an estrogen receptor-negative, highly proliferative breast carcinoma subtype. Breast cancer research and treatment. 2006; 98: 91–98. doi: 10.1007/s10549-005-9135-2 PMID: 16636895

22. Barbareschi M, Maisonneuve P, Aldovini D, Cangi MG, Pecciarini L, Angelo Mauri F, et al. High syndecan-1 expression in breast carcinoma is related to an aggressive phenotype and to poorer prognosis. Cancer. 2003; 98: 474–483. doi: 10.1002/cncr.11515 PMID: 12879463

23. Götte M, Kersting C, Radke I, Kiesel L, Wülfing P. An expression signature of syndecan-1 (CD138), E-cadherin and c-met is associated with factors of angiogenesis and lymphangiogenesis in ductal breast carcinoma in situ. Breast Cancer Res. 2007; 9: R8. doi: 10.1186/bcr1641 PMID: 17244359

24. Hashimoto Y, Skacel M, Adams JC. Association of loss of epithelial syndecan-1 with stage and local metastasis of colorectal adenocarcinomas: an immunohistochemical study of clinically annotated tumors. BMC Cancer. 2008; 8: 185. doi: 10.1186/1471-2407-8-185 PMID: 18590537

25. Yang N, Mosher R, Seo S, Beebe D, Friedl A. Syndecan-1 in breast cancer stroma fibroblasts regulates extracellular matrix fiber organization and carcinoma cell motility. Am J Pathol. 2011; 178: 325–335. doi: 10.1016/j.ajpath.2010.11.039 PMID: 21224069

26. Stanley MJ, Stanley MW, Sanderson RD, Zera R. Syndecan-1 expression is induced in the stroma of infiltrating breast carcinoma. Am J Clin Pathol. 1999; 112: 377–383. PMID: 10478144

27. Maeda T, Alexander CM, Friedl A. Induction of syndecan-1 expression in stromal fibroblasts promotes proliferation of human breast cancer cells. Cancer research. 2004; 64: 612–621. PMID: 14744776

28. Langford JK, Stanley MJ, Cao D, Sanderson RD. Multiple heparan sulfate chains are required for optimal syndecan-1 function. J Biol Chem. 1998; 273: 29965–29971. PMID: 9792716

29. McQuade KJ, Rapraeger AC. Syndecan-1 transmembrane and extracellular domains have unique and distinct roles in cell spreading. J Biol Chem. 2003; 278: 46607–46615. doi: 10.1074/jbc.M304775200 PMID: 12975379

30. Lebakken CS, Rapraeger AC. Syndecan-1 mediates cell spreading in transfected human lymphoblastoid (Raji) cells. J Cell Biol. The Rockefeller University Press; 1996; 132: 1209–1221.

31. Beauvais DM, Rapraeger AC. Syndecans in tumor cell adhesion and signaling. Reprod Biol Endocrinol. 2004; 2: 3. doi: 10.1186/1477-7827-2-3 PMID: 14711376

32. Beauvais DM, Ell BJ, McWhorter AR, Rapraeger AC. Syndecan-1 regulates alphavbeta3 and alphavbeta5 integrin activation during angiogenesis and is blocked by synstatin, a novel peptide inhibitor. J Exp Med. 2009; 206: 691–705. doi: 10.1084/jem.20081278 PMID: 19255147

33. Altemeier WA, Schlesinger SY, Buell CA, Brauer R, Rapraeger AC, Parks WC, et al. Transmembrane and extracellular domains of syndecan-1 have distinct functions in regulating lung epithelial migration and adhesion. Journal of Biological Chemistry. 2012; 287: 34927–34935. doi: 10.1074/jbc.M112.376814 PMID: 22936802

34. Beauvais DM, Rapraeger AC. Syndecan-1 couples the insulin-like growth factor-1 receptor to inside-out integrin activation. J Cell Sci. 2010; 123: 3796–3807. doi: 10.1242/jcs.067645 PMID: 20971705

35. McQuade KJ, Beauvais DM, Burbach BJ, Rapraeger AC. Syndecan-1 regulates alphavbeta5 integrin activity in B82L fibroblasts. J Cell Sci. 2006; 119: 2445–2456. doi: 10.1242/jcs.02970 PMID: 16720645

36. Rapraeger AC. Synstatin: a selective inhibitor of the syndecan-1-coupled IGF1R–αvβ3 integrin complex in tumorigenesis and angiogenesis. FEBS J. 2013; 280: 2207–2215. doi: 10.1111/febs.12160 PMID: 23375101

37. Fogerty FJ, Mosher DF. Mechanisms for organization of fibronectin matrix. Cell Differ Dev. 1990; 32: 439–450. PMID: 2151569

38. Mao Y, Schwarzbauer JE. Accessibility to the fibronectin synergy site in a 3D matrix regulates engagement of alpha5beta1 versus alphavbeta3 integrin receptors. Cell Commun Adhes. 2006; 13: 267–277. doi: 10.1080/15419060601072215 PMID: 17162669

39. Singh P, Carraher C, Schwarzbauer JE. Assembly of fibronectin extracellular matrix. Annu Rev Cell Dev Biol. 2010; 26: 397–419. doi: 10.1146/annurev-cellbio-100109-104020 PMID: 20690820

40. Wu C, Hughes PE, Ginsberg MH, McDonald JA. Identification of a new biological function for the integrin alpha v beta 3: initiation of fibronectin matrix assembly. Cell Adhes Commun. 1996; 4: 149–158. PMID: 8969861

41. Yang JT, Hynes RO. Fibronectin receptor functions in embryonic cells deficient in alpha 5 beta 1 integrin can be replaced by alpha V integrins. Mol Biol Cell. 1996; 7: 1737–1748. PMID: 8930896

42. Hynes RO. Integrins: bidirectional, allosteric signaling machines. Cell. 2002; 110: 673–687. PMID: 12297042

43. Miller FR, Santner SJ, Tait L, Dawson PJ. MCF10DCIS.com xenograft model of human comedo ductal carcinoma in situ. J Natl Cancer Inst. 2000; 92: 1185–1186.

44. Wu C, Keivens VM, O'Toole TE, McDonald JA, Ginsberg MH. Integrin activation and cytoskeletal interaction are essential for the assembly of a fibronectin matrix. Cell. 1995; 83: 715–724. PMID: 8521488

45. Vomund AN, Stuhlsatz-Krouper S, Dimitry J, Song Y, Frazier WA. A naturally occurring extracellular alpha-beta clasp contributes to stabilization of beta3 integrins in a bent, resting conformation. Biochemistry. 2008; 47: 11616–11624. doi: 10.1021/bi8015108 PMID: 18841997

46. Kusano Y, Yoshitomi Y, Munesue S, Okayama M, Oguri K. Cooperation of syndecan-2 and syndecan-4 among cell surface heparan sulfate proteoglycans in the actin cytoskeletal organization of Lewis lung carcinoma cells. J Biochem. 2004; 135: 129–137. PMID: 14999018

47. Leppä S, Mali M, Miettinen HM, Jalkanen M. Syndecan expression regulates cell morphology and growth of mouse mammary epithelial tumor cells. Proceedings of the National Academy of Sciences of the United States of America. National Academy of Sciences; 1992; 89: 932–936.

48. Lim HC, Couchman JR. Syndecan-2 regulation of morphology in breast carcinoma cells is dependent on RhoGTPases. Biochim Biophys Acta. 2014; 1840: 2482–2490. doi: 10.1016/j.bbagen.2014.01.018 PMID: 24447566

49. Calderwood DA, Shattil SJ, Ginsberg MH. Integrins and actin filaments: reciprocal regulation of cell adhesion and signaling. J Biol Chem. American Society for Biochemistry and Molecular Biology; 2000; 275: 22607–22610. doi: 10.1074/jbc.R900037199 PMID: 10801899

50. Versaevel M, Grevesse T, Gabriele S. Spatial coordination between cell and nuclear shape within micropatterned endothelial cells. Nat Commun. 2012; 3: 671. doi: 10.1038/ncomms1668 PMID: 22334074

51. Khatau SB, Hale CM, Stewart-Hutchinson PJ, Patel MS, Stewart CL, Searson PC, et al. A perinuclear actin cap regulates nuclear shape. Proceedings of the National Academy of Sciences of the United States of America. National Acad Sciences; 2009; 106: 19017–19022. doi: 10.1073/pnas.0908686106

52. Provenzano PP, Inman DR, Eliceiri KW, Knittel JG, Yan L, Rueden CT, et al. Collagen density promotes mammary tumor initiation and progression. BMC Med. 2008; 6: 11. doi: 10.1186/1741-7015-6-11 PMID: 18442412

53. Paszek MJ, Zahir N, Johnson KR, Lakins JN, Rozenberg GI, Gefen A, et al. Tensional homeostasis and the malignant phenotype. Cancer Cell. 2005; 8: 241–254. doi: 10.1016/j.ccr.2005.08.010 PMID: 16169468

54. Conklin MW, Eickhoff JC, Riching KM, Pehlke CA, Eliceiri KW, Provenzano PP, et al. Aligned collagen is a prognostic signature for survival in human breast carcinoma. Am J Pathol. 2011; 178: 1221–1232. doi: 10.1016/j.ajpath.2010.11.076 PMID: 21356373

55. Amatangelo MD, Bassi DE, Klein-Szanto AJP, Cukierman E. Stroma-derived three-dimensional matrices are necessary and sufficient to promote desmoplastic differentiation of normal fibroblasts. Am J Pathol. 2005; 167: 475–488. doi: 10.1016/S0002-9440(10)62991-4 PMID: 16049333

56. Dumont N, Liu B, Defilippis RA, Chang H, Rabban JT, Karnezis AN, et al. Breast fibroblasts modulate early dissemination, tumorigenesis, and metastasis through alteration of extracellular matrix characteristics. NEO. 2013; 15: 249–262.

57. Maller O, Hansen KC, Lyons TR, Acerbi I, Weaver VM, Prekeris R, et al. Collagen architecture in pregnancy-induced protection from breast cancer. J Cell Sci. 2013; 126: 4108–4110. doi: 10.1242/jcs.121590 PMID: 23843613

58. Klass CM, Couchman JR, Woods A. Control of extracellular matrix assembly by syndecan-2 proteoglycan. J Cell Sci. 2000; 113 (Pt 3): 493–506. PMID: 10639336

59. Wierzbicka-Patynowski I, Schwarzbauer JE. The ins and outs of fibronectin matrix assembly. J Cell Sci. 2003; 116: 3269–3276. doi: 10.1242/jcs.00670 PMID: 12857786

60. Stepp MA, Pal-Ghosh S, Tadvalkar G, Rajjoub L, Jurjus RA, Gerdes M, et al. Loss of syndecan-1 is associated with malignant conversion in skin carcinogenesis. Mol Carcinog. 2010; 49: 363–373. doi: 10.1002/mc.20609 PMID: 20082322

61. Lee H- O, Mullins SR, Franco-Barraza J, Valianou M, Cukierman E, Cheng JD. FAP-overexpressing fibroblasts produce an extracellular matrix that enhances invasive velocity and directionality of pancreatic cancer cells. BMC Cancer. BioMed Central Ltd; 2011; 11: 245. doi: 10.1186/1471-2407-11-245

62. Goetz JG, Minguet S, Navarro-Lérida I, Lazcano JJ, Samaniego R, Calvo E, et al. Biomechanical remodeling of the microenvironment by stromal caveolin-1 favors tumor invasion and metastasis. Cell. 2011; 146: 148–163. doi: 10.1016/j.cell.2011.05.040 PMID: 21729786

63. Beauvais DM, Rapraeger AC. Syndecan-1-mediated cell spreading requires signaling by alphavbeta3 integrins in human breast carcinoma cells. Experimental cell research. 2003; 286: 219–232. PMID: 12749851

64. Calderwood DA, Zent R, Grant R, Rees DJ, Hynes RO, Ginsberg MH. The Talin head domain binds to integrin beta subunit cytoplasmic tails and regulates integrin activation. J Biol Chem. 1999; 274: 28071–28074. PMID: 10497155

65. Schwarzbauer JE, DeSimone DW. Fibronectins, their fibrillogenesis, and in vivo functions. Cold Spring Harb Perspect Biol. 2011; 3. doi: 10.1101/cshperspect.a005041

66. Leiss M, Beckmann K, Girós A, Costell M, Fässler R. The role of integrin binding sites in fibronectin matrix assembly in vivo. Curr Opin Cell Biol. 2008; 20: 502–507. doi: 10.1016/j.ceb.2008.06.001 PMID: 18586094

67. Mao Y, Schwarzbauer JE. Fibronectin fibrillogenesis, a cell-mediated matrix assembly process. Matrix Biol. 2005; 24: 389–399. doi: 10.1016/j.matbio.2005.06.008 PMID: 16061370

68. Tumova S, Woods A, Couchman JR. Heparan sulfate chains from glypican and syndecans bind the Hep II domain of fibronectin similarly despite minor structural differences. J Biol Chem. 2000; 275: 9410–9417. PMID: 10734086

69. Woods A, Longley RL, Tumova S, Couchman JR. Syndecan-4 binding to the high affinity heparin-binding domain of fibronectin drives focal adhesion formation in fibroblasts. Arch Biochem Biophys. 2000; 374: 66–72. doi: 10.1006/abbi.1999.1607 PMID: 10640397

70. Pankov R, Yamada KM. Fibronectin at a glance. J Cell Sci. 2002; 115: 3861–3863. PMID: 12244123

71. Bloom L, Ingham KC, Hynes RO. Fibronectin regulates assembly of actin filaments and focal contacts in cultured cells via the heparin-binding site in repeat III13. Mol Biol Cell. 1999; 10: 1521–1536. PMID: 10233160

72. Johnson KJ, Sage H, Briscoe G, Erickson HP. The compact conformation of fibronectin is determined by intramolecular ionic interactions. J Biol Chem. 1999; 274: 15473–15479. PMID: 10336438

73. Wu C, Bauer JS, Juliano RL, McDonald JA. The alpha 5 beta 1 integrin fibronectin receptor, but not the alpha 5 cytoplasmic domain, functions in an early and essential step in fibronectin matrix assembly. J Biol Chem. 1993; 268: 21883–21888. PMID: 7691819

74. Wennerberg K, Lohikangas L, Gullberg D, Pfaff M, Johansson S, Fässler R. Beta 1 integrin-dependent and -independent polymerization of fibronectin. J Cell Biol. 1996; 132: 227–238. PMID: 8567726

75. Aota S, Nomizu M, Yamada KM. The short amino acid sequence Pro-His-Ser-Arg-Asn in human fibronectin enhances cell-adhesive function. J Biol Chem. 1994; 269: 24756–24761. PMID: 7929152

76. Bowditch RD, Hariharan M, Tominna EF, Smith JW, Yamada KM, Getzoff ED, et al. Identification of a novel integrin binding site in fibronectin. Differential utilization by beta 3 integrins. J Biol Chem. 1994; 269: 10856–10863. PMID: 7511609

77. Curnis F, Longhi R, Crippa L, Cattaneo A, Dondossola E, Bachi A, et al. Spontaneous formation of L-isoaspartate and gain of function in fibronectin. J Biol Chem. 2006; 281: 36466–36476. doi: 10.1074/jbc.M604812200 PMID: 17015452

78. Danen EH, Aota S, van Kraats AA, Yamada KM, Ruiter DJ, van Muijen GN. Requirement for the synergy site for cell adhesion to fibronectin depends on the activation state of integrin alpha 5 beta 1. J Biol Chem. 1995; 270: 21612–21618. PMID: 7545166

79. Friman T, Gustafsson R, Stuhr LB, Chidiac J, Heldin N- E, Reed RK, et al. Increased fibrosis and interstitial fluid pressure in two different types of syngeneic murine carcinoma grown in integrin β3-subunit deficient mice. PloS one. 2012; 7: e34082. doi: 10.1371/journal.pone.0034082 PMID: 22479530

80. Kuperwasser C, Chavarria T, Wu M, Magrane G, Gray JW, Carey L, et al. Reconstruction of functionally normal and malignant human breast tissues in mice. Proceedings of the National Academy of Sciences of the United States of America. 2004; 101: 4966–4971. doi: 10.1073/pnas.0401064101 PMID: 15051869

81. Cukierman E, Pankov R, Yamada KM. Cell interactions with three-dimensional matrices. Curr Opin Cell Biol. 2002; 14: 633–639. PMID: 12231360